Optimal strokes at low Reynolds number: a geometric and numeric study using the Copepod and Purcell swimmers

P Bettiol, B Bonnard, J Rouot

Optimal strokes at low Reynolds number: a geometric and numeric study using the Copepod and Purcell swimmers.

P. Bettiol *

Laboratoire de Mathématiques Unité CNRS UMR 6205, Université de Bretagne Occidentale, 6, Avenue Victor Le Gorgeu, 29200 Brest, France

B. Bonnard †

Inria Sophia Antipolis et Institut de Mathématiques de Bourgogne, 9 avenue Savary, 21078 Dijon, France

J. Rouot ‡

Inria Sophia Antipolis, 2004 route des lucioles, F-06902 Sophia Antipolis, France

In this article, we make a comparative geometric and numeric analysis of the optimal strokes at low Reynolds number using two specific rigid links swimmers: the Copepod swimmer, a symmetric swimmer introduced recently[28] and the historical three-link Purcell swimmer[25] where the cost to minimize is the mechanical power dissipated by the fluid's viscous drag forces. This leads to a sub-Riemannian problem which can be analyzed in this rich framework. In particular nilpotent approximation can be used to compute strokes with small amplitudes and they can be continued to compute numerically more general strokes. The concept of geometric efficiency corresponding to the ratio between the displacement and the length of the stroke is introduced to analyze the global optimality. The role of both abnormal and normal strokes is described, in particular in the symmetric case, in relation with observed motions of the microorganisms. Moreover C^1-optimality is studied using the concept of conjugate points, depending upon their respective shapes. In parallel direct and indirect numerical schemes implemented in the `Bocop` (`www.bocop.org`,[6]) and `HamPath` softwares (`www.hampath.org`,[14]) allow to perform numerical simulations, crucial to complete theoretical study and to evaluate the optimal solutions.

Keywords: Low Reynolds number, Copepod swimmer, Purcell swimmer, SR-geometry, periodic optimal control, second order optimality conditions.

AMS Subject Classification: 49K15, 93C10, 70Q05

1. Introduction

Swimming models at low Reynolds numbers applicable to microorganisms and restricting to rigid links has been introduced in the fifties[25] and assuming that the

*piernicola.bettiol@univ-brest.fr
†bernard.bonnard@u-bourgogne.fr
‡jeremy.rouot@inria.fr

displacement is performed minimizing the mechanical power dissipated by the drag forces, the optimal strokes can be determined in the framework of SR-geometry. This area has recently produced a lot of useful results in our study, e.g. the concept of nilpotent approximation[3] and explicit computations of the spheres with small radius[8] to parameterize and analyze strokes with small amplitudes, the role of normal and abnormal geodesics[21,11] and smoothness of the minimizers[26], computations of conjugate points in relation with C^1-optimality in the normal and abnormal case[8,1].
Also the concept of optimal strokes is related to periodic optimal control and is connected to the standard problem of finding periodic solutions of the Hamiltonian vector fields introduced by Poincaré in relation with the N-body problem[24] and well studied by this contributor using continuation and variational methods: existence of one-parameter family of periodic trajectory emanating from an equilibrium point[23], direct methods to compute periodic solutions, in relation with the class of homotopy related to collisions. All contributions valuable to direct and indirect numerical schemes like in the `Bocop` and `HamPath` softwares and understanding the shape of the optimal strokes related to the singular configurations of the n-link swimmer.

Altogether the problem boils down to generate multi-parameters family of periodic solutions whose optimality can be analyzed C^1-locally using the concept of conjugate points[8,2], the concept of focal point taking into account non uniqueness of minimizers[29] or globally with the concept of geometric efficiency, a simplification of the concept of efficiency of a swimmer[19].

The organization of this article is the following. In section 2, due to space restrictions, we present briefly the concepts and results needed in our study. First of all the model[16] of swimming at low Reynolds number is specialized to the case of a n-links swimmer is standard and leads easily to the dynamical model and the explicit form of the equations[22]. Secondly we recall elements of SR-geometry and introduce the concept of geometric efficiency. Finally the two softwares (`Bocop` and `HamPath`) and their use in our numerical computations are presented. The section 3 presents the combination of our geometric and numeric analysis to determine optimal strokes of the Copepod swimmer. This case is very important in our study: it is a model of swimmers of an abundant variety of zooplankton which can be observed, it will be used in the future to design a micro-robot to validate our computations. Moreover the model leads to tractable Lie brackets computations, state constraints form a triangle and has a nice geometric interpretation. As a dynamical model it is sufficiently complex to generate a variety of different strokes in accordance with the classification of periodic planar curves[4]. Finally C^1-optimality can be analyzed using the concept of conjugate points and the concept of geometric efficiency allows to finalize the study. The section 4 is devoted to the three-link Purcell swimmer. The nilpotent approximation is determined to evaluate analytically the strokes with small amplitudes, thanks to integrability. Numeric computations using `Bocop` and `HamPath` softwares allow to compute more general strokes and to test their optimality with dedicated algorithms to compute conjugate points in the normal and

abnormal case, and focal points to deal with symmetry properties.

2. Generalities

2.1. *The mathematical model*

In this section, we present briefly the mathematical models, the complete equations in the case of n-links can being explicitly given[22]. The two swimmers are represented in Fig.1, with the corresponding state variables:

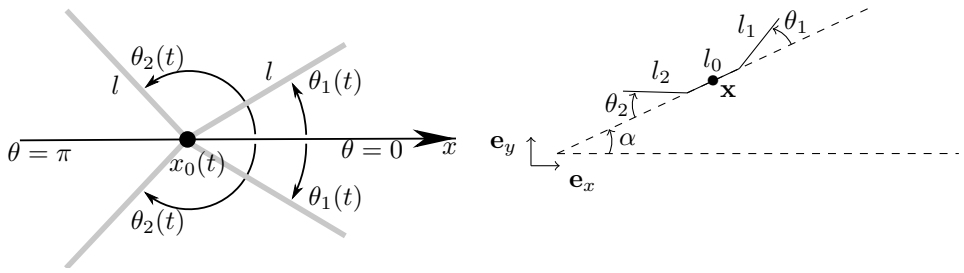

Fig. 1: *(left)* Copepod swimmer, *(right)* Purcell swimmer.

Copepod swimmer: it is formed by gluing together two scallops. Each pair of symmetric links have some length normalized to $l = 1$.
The swimming velocity at x_0 is given by[28]:

$$\dot{x_0} = \frac{\dot{\theta}_1 \sin(\theta_1) + \dot{\theta}_2 \sin(\theta_2)}{2 + \sin^2(\theta_1) + \sin^2(\theta_2)} \tag{2.1}$$

and denoting $\theta = (\theta_1, \theta_2)$ and $\dot{\theta} = u = (u_1, u_2)$ we have

$$\dot{\theta} = u = H_1(\theta)\tau \tag{2.2}$$

where τ is the drag force. The mechanical power is given by a positive quadratic form $\dot{q}^\intercal M(q)\dot{q}$, $q = (x_0, \theta)$ where

$$M = \begin{pmatrix} 2 - 1/2(\cos^2(\theta_1) + \cos^2(\theta_2)) & -1/2\sin(\theta_1) & -1/2\sin(\theta_2) \\ -1/2\sin(\theta_1) & 1/3 & 0 \\ -1/2\sin(\theta_2) & 0 & 1/3 \end{pmatrix}$$

and using (2.1) this amounts to minimize the quadratic cost:

$$\int_0^T \left(a(q)u_1^2 + 2b(q)u_1u_2 + c(q)u_2^2\right) \mathrm{d}t \tag{2.3}$$

with

$$a = \frac{1}{3} - \frac{\sin^2\theta_1}{2(2+\sin^2\theta_1+\sin^2\theta_2)},$$
$$b = -\frac{\sin\theta_1\sin\theta_2}{2(2+\sin^2\theta_1+\sin^2\theta_2)},$$
$$c = \frac{1}{3} - \frac{\sin^2\theta_2}{2(2+\sin^2\theta_1+\sin^2\theta_2)}.$$

Purcell swimmer: the model is much more complex. Denoting $q = (x, y, \alpha, \theta_1, \theta_2)$ it takes the form:

$$\begin{pmatrix}\dot{x}\\ \dot{y}\\ \dot{\alpha}\end{pmatrix} = \frac{1}{\Delta G} R \begin{pmatrix} g_{11} & g_{12}\\ g_{21} & g_{22}\\ g_{31} & g_{32}\end{pmatrix}\begin{pmatrix}\dot{\theta_1}\\ \dot{\theta_2}\end{pmatrix}, \qquad (2.4)$$
$$\dot{\theta} = u = H_2(\theta)\tau,$$

where R is the rotation matrix

$$R = \begin{pmatrix}\cos(\alpha) & -\sin(\alpha) & 0\\ \sin(\alpha) & \cos(\alpha) & 0\\ 0 & 0 & 1\end{pmatrix}$$

where g_{ij}, ΔG and $H_2(\theta)$ are detailed,[22] (two pages). Again the cost function u is minimizing the expanded mechanical power

$$\int_0^T \tau \cdot u \, \mathrm{d}t.$$

We use the following terminology.

Definition 2.1. The two angular variables $\theta = (\theta_1, \theta_2)$ are called the *shape variables*. A *stroke* of period T consists in a periodic motion in the shape variables.

State constraints Note that the design of the corresponding system will produce state constraints:

- Copepod case. One has :

$$\theta_1, \theta_2 \in [0, \pi],\ \theta_1 \leq \theta_2$$

- Purcell case. They depend upon the assumption about the length l_0 of the body and the respective lengths l_1, l_2 of the leg and the arms. We shall perform our computations assuming $l_0 = 2$ and $l_1 = l_2 = 1$. Hence we have the amplitude bounds: $\theta_1, \theta_2 \in [-\pi, \pi]$.

2.2. *Elements of sub-Riemannian geometry*

The optimal control problem is written

$$\dot{q} = \sum_{i=1}^{2} u_i G_i(q), \quad \min_{u(.)} \int_0^T (u^\intercal R(q) u)\, \mathrm{d}t,$$

where the set of admissible controls $\mathcal{U}$ is the set of bounded measurable mappings. Note that T can be fixed to 2π. The *length* of a control trajectory is

$$l(q) = \int_0^T (u^\intercal R(q) u)^{1/2}\, \mathrm{d}t$$

Using the standard concepts of sub-Riemannian geometry,[17] we introduce the following.

Definition 2.2. Let D be the distribution $\mathrm{span}\{G_1, G_2\}$. Using a feedback transformation $u = \beta(q)v$, we may choose locally an *orthonormal* frame $F = (F_1, F_2)$ such that the cost function reduces to $v^\intercal v$. Near a point q_0, one can choose the so-called *privileged coordinates* so that the distribution D can be approximated by a *nilpotent distribution* denoted $\widehat{D} = \mathrm{span}\{\widehat{G_1}, \widehat{G_2}\}$. Similarly, one can choose an *nilpotent orthonormal* frame denoted $\{\widehat{F_1}, \widehat{F_2}\}$ to approximate the SR-problem.

Note that this approximation step is particularly important in the Purcell case where the complexity of the model leads to non realizable analytic computations.

2.2.1. *Maximum Principle and computations of geodesic equations*

The Maximum Principle is used to compute the geodesic equations. Denoting $z = (q, p)$ the symplectic coordinates and $H_F(z) = p \cdot F(q)$ the Hamiltonian lift of the vector field F. Assuming that $\{F_1, F_2\}$ forms an orthonormal frame, the pseudo-Hamiltonian takes the form:

$$H(z, u) = \sum_{i=1}^{2} u_i H_i(z) + \lambda_0 \sum_{i=1}^{2} u_i^2$$

where H_i is the Hamiltonian lift of F_i and λ_0 is a constant which can be normalized to $\lambda_0 = -1/2$ (*normal case*) or $\lambda_0 = 0$ (*abnormal case*). Using the condition: $\frac{\partial H}{\partial u} = 0$ one gets the two cases.

- Normal case: We get $u_i = H_i$ and plugging such u_i into H leads to the true Hamiltonian in the normal case: $H_n = \frac{1}{2}\sum_{i=1}^{2} H_i^2$. The corresponding solutions are called *normal extremals* and their projections on the q-space are called *normal geodesics*.
- Abnormal case: We get the constraints $H_i(z) = 0$, $i = 1, 2$. The corresponding solutions are called *abnormal extremals* and their projections are called *abnormal geodesics*.

This leads to the following concepts.

Definition 2.3. Assuming arc-length parameterization $H_n = 1/2$, the *exponential mapping* is: $\exp_{q_0} : (t, p(0)) \to \Pi(\exp(t\overrightarrow{H_n}(z(0))))$, with $z(0) = (q_0, p(0))$ and Π is the projection: $z \mapsto q$. A *conjugate time* (normal case) is a time t_c such that the function $\exp_{q_0}$ is not of full rank at t_c and the corresponding point is called a *conjugate point* along the geodesic with initial condition $z(0)$. We denote t_{1c} the *first conjugate point*.

2.2.2. *Concepts of SR-geometry dedicated to the swimmer problem*

Two aspects of the problem are the state constraints which will be no theoretically studied in this article and the boundary conditions related to strokes which will be introduced next.

Boundary conditions associated to periodicity We split the state variables q into (q_1, q_2) and let $p = (p_1, p_2)$ be the associated splitting of the adjoint vector. Assuming periodic conditions: $q_2(0) = q_2(T)$ the Maximum Principle leads to the condition:

$$p_2(0) = p_2(T) \tag{2.5}$$

Definition 2.4. A *normal* (resp. *abnormal*) *stroke* is a stroke corresponding to a normal (resp. abnormal) extremal. A *piecewise smooth abnormal stroke* is a piecewise smooth stroke such that each smooth sub-arc corresponds to an abnormal arc.

Shooting equation To define the *shooting equation*: S, one restricts the flow to normal extremals, solution of $\overrightarrow{H_n}$, with the following boundary conditions associated to the state variables splitting:

- $q_1(0) = q_1^0, q_1(T) = q_1^T$ where q_1^0, q_1^T are fixed,
- $q_2(0) = q_2(T)$, $p_1(0) = p_1(T)$

Observe that this leads to non unique solutions due to invariance with respect to time of the periodic solution. But this ambiguity can be removed by choosing a *section* Σ to the periodic solution.

In the framework of SR-geometry and in relation with the underlying fixed extremities we have the following[8,1].

Property 2.1. The shooting mapping fails to be locally injective due to the existence of conjugate points.

Property 2.2. The shooting mapping fails to be proper due to the existence of abnormal extremals.

Finally in relation with the problem we introduce the following concept.

Definition 2.5. The *geometric efficiency* $\mathcal{E}$ of a stroke γ is defined as

- Copepod swimmer: $\mathcal{E} = x_0(T)/l(\gamma)$,
- Purcell swimmer: $\mathcal{E} = \sqrt{x(T)^2 + y(T)^2}/l(\gamma)$

that is the ratio between the euclidean displacement and the sub-Riemannian length of the stroke.

2.2.3. *Standard concepts*

Finally we recall the standard concepts of SR-geometry related to the problem with fixed extremities. Having fixed $q(0) = q_0$, the *conjugate locus* $\mathcal{C}(q_0)$ is the set of first conjugate points considering all normal geodesics emanating from q_0. The *cut locus* $C_\Sigma(q_0)$ is the set of points where a (normal or abnormal) geodesic emanating from q_0 ceases to be optimal. The *sphere* $S(q_0, r)$ is formed by the set of points at SR-distance r from q_0.

2.3. *Bocop and HamPath softwares*

- `Bocop` . The so-called direct approach transforms an infinite dimensional control into a finite dimensional optimization problem. This is done by a discretisation in time applied to the state space, control variables and the dynamics. This method can take into accounts control and state variables constraints. Less precise that the indirect method based on the Maximum Principle, but most robust with respect to the initialization. It will use to compute optimal strokes satisfying the state constraints and also as a complementary method to initialize the shooting of the direct method implemented in `HamPath`
- `HamPath` This software is based upon indirect methods and solve the shooting equation and differential continuation (homotopy) methods and computation of the solutions of the variational equation to check second order conditions of local optimality (conjugate points computations). Having found a stroke using nilpotent approximations and explicit computations (for small amplitudes) or more general solution using `Bocop`, a continuation is performed mainly using as parameter the displacement.

3. The Copepod swimmer

3.1. *Preliminary results*

3.1.1. *A geometric analysis*

First of all we recall two types of geometric strokes,[28] and which will be the motivation of our study.

First case (Fig.2) The two legs are assumed to oscillate sinusoidally with period 2π according to

$$\theta_1 = \Phi_1 + a\cos(t), \quad \theta_2 = \Phi_2 + a\cos(t + k_2)$$

with $a = \pi/4$, $\Phi_1 = \pi/4$, $\Phi_2 = 3\pi/4$ and $k_2 = \pi/2$, such parameters being chosen to optimize this efficiency. Assuming $x_0(0) = 0$, this produces a displacement $x_0(2\pi) = 0.2$.
Parameters a, Φ_1, Φ_2 and k are designed to maximize the efficiency.

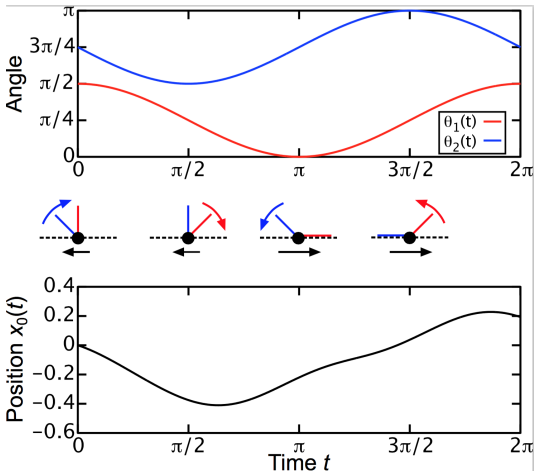

Fig. 2: Two legs oscillating sinusoidally according to $\theta_1 = \pi/4 + a\cos t$ and $\theta_2 = 3\pi/4 + a\cos(t + \pi/2)$, where $a = \pi/4$ is the amplitude. The second leg (blue) oscillates about $\Phi_2 = 3\pi/4$, while the first leg (red) oscillates about $\Phi_1 = \pi/4$ with a phase lag of $\pi/2$. The swimmer position x_0 translates about a fifth of the leg length after one cycle.

Second case (Fig.3) The two legs are paddling in sequence followed by a recovery stroke performed in unison. In this case, the first step is to steer θ_1 follows by θ_2 from 0 to π, while the unison sequence corresponds to a displacement from π to 0 with the constraint $\theta_1 = \theta_2$. Note it corresponds to a *triangle stroke* and moreover θ_1 and θ_2 stay in the boundary of the domain.

3.1.2. *Abnormal curves in the copepod swimmer*

With $q = (x_0, \theta_1, \theta_2) \in \mathbb{R}^3$, the dynamics given by the control system

$$\dot{q}(t) = \sum_{i=1}^{2} u_i(t) G_i(q(t)).$$

The Lie bracket of two vectors fields F, G is computed with the convention

$$[F, G](q) = \frac{\partial F}{\partial q}(q)G(q) - \frac{\partial G}{\partial q}(q)F(q).$$

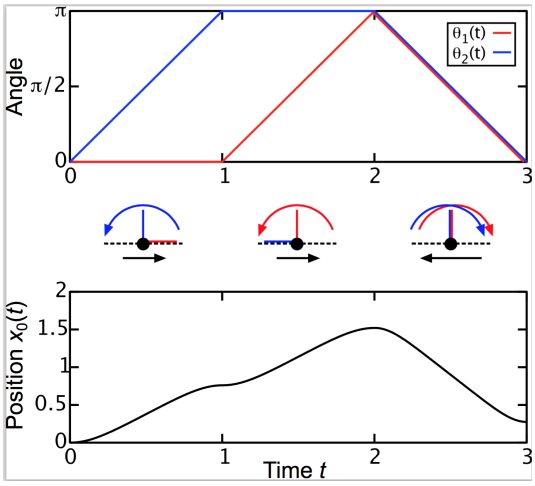

Fig. 3: Two legs paddling in sequence. The legs perform power strokes in sequence and then a recovery stroke in unison, each stroke sweeping an angle π.

Denoting $p = (p_1, p_2, p_3)$ the adjoint vector associated with q, $z = (q, p)$ and if H_F, H_G are the Hamiltonian lifts $p \cdot F, p \cdot G$, one has:

$$\{H_F, H_G\}(z) = \mathrm{d}H_F(\overrightarrow{H}_G)(z) = p \cdot [F, G](q).$$

Denoting $D = \mathrm{span}\{G_1, G_2\}$, the distribution associated to the control system, one needs to recall basics facts about the classification of such two-dimensional distributions, in relation with abnormal curves,[30].

Local classification of two-dimensional distributions in dimension three and abnormal curves Denoting $H_i(z) = p \cdot G_i(q)$ $i = 1, 2$ the Hamiltonian lifts, abnormal curves are defined by

$$H_1(z) = H_2(z) = 0$$

and differentiating using the dynamics

$$\frac{\mathrm{d}z}{\mathrm{d}t} = \sum_{i=1}^{2} u_i \overrightarrow{H}_i(z)$$

we obtain the relations

$$\{H_1, H_2\}(z) = 0$$
$$u_1 \{\{H_1, H_2\}, H_1\}(z) + u_2 \{\{H_1, H_2\}, H_2\}(z) = 0$$

defining the corresponding abnormal controls. Next, we present only the two stable models related to our study.

Contact case. We say that q_0 is a *contact point* if $\{G_1, G_2, [G_1, G_2]\}$ is of dimension

3 at q_0. At a contact point, identified to 0, there exists a system of local coordinates $q = (x, y, z)$ such that

$$D = \ker(\alpha), \qquad \alpha = \mathrm{d}z + (x\mathrm{d}y + y\mathrm{d}x).$$

with the corresponding nilpotent frame

$$\widehat{G_1} = \frac{\partial}{\partial x} + y\frac{\partial}{\partial z}, \widehat{G_2} = \frac{\partial}{\partial y} - x\frac{\partial}{\partial z}$$

Taking $\widehat{G_1}, \widehat{G_2}$ as an orthonormal frame, this leads to the *Heisenberg model* in SR-geometry. Observe that $\mathrm{d}\alpha = \mathrm{d}y \wedge \mathrm{d}x$ (Darboux form) and that $\frac{\partial}{\partial z}$ is the characteristic direction of $\mathrm{d}\alpha$.

The Martinet case. A point q_0 is a *Martinet point* if at q_0, $[G_1, G_2] \in D = \mathrm{span}\{G_1, G_2\}$ and at least one Lie bracket $[[G_1, G_2], G_1]$ or $[[G_1, G_2], G_2]$ does not belong to D. Then, there exist local coordinates $q = (x, y, z)$ near q_0 identified to 0 such that

$$D = \ker \omega, \qquad \omega = \mathrm{d}z - \frac{y^2}{2}\mathrm{d}x$$

and the corresponding nilpotent frame

$$\widehat{G_1} = \frac{\partial}{\partial x} + \frac{y^2}{2}\frac{\partial}{\partial z}, \widehat{G_2} = \frac{\partial}{\partial y}.$$

Moreover

$$\widehat{G_3} = [\widehat{G_1}, \widehat{G_2}] = y\frac{\partial}{\partial z}, \ [[\widehat{G_1}, \widehat{G_2}], \widehat{G_1}] = 0, \ [[\widehat{G_1}, \widehat{G_2}], \widehat{G_2}] = \frac{\partial}{\partial z}. \tag{3.1}$$

The surface $\Sigma : y = 0$ where $\widehat{G_1}, \widehat{G_2}, [\widehat{G_1}, \widehat{G_2}]$ are linearly dependant is called the *Martinet surface* and is foliated by abnormal curves, solutions of $\frac{\partial}{\partial x}$. In particular, through the origin it corresponds to the curve $t \to (t, 0, 0)$. Taking $\widehat{G_1}, \widehat{G_2}$ as an orthonormal frame, it corresponds to the so-called *flat Martinet case*.

Computation in the Copepod case One has

$$G_i = \frac{\sin(\theta_i)}{\Delta}\frac{\partial}{\partial x_0} + \frac{\partial}{\partial \theta_i}, \ i = 1, 2 \ , \Delta = 2 + \sin^2(\theta_1) + \sin^2(\theta_2).$$

and

$$G_3 = [G_1, G_2] = f(\theta_1, \theta_2)\frac{\partial}{\partial x_0}$$

with

$$f(\theta_1, \theta_2) = \frac{2\sin(\theta_1)\sin(\theta_2)(\cos(\theta_1) - \cos(\theta_2))}{\Delta^2},$$
$$[[G_1, G_2], G_i] = \frac{\partial f}{\partial \theta_i}(\theta_1, \theta_2)\frac{\partial}{\partial x_0}, \ i = 1, 2.$$

and we deduce

Lemma 3.1. *The Martinet surface* Σ *where the vector fields* $G_1, G_2, [G_1, G_2]$ *are coplanar, is given by* $2\sin(\theta_1)\sin(\theta_2)(\cos(\theta_1) - \cos(\theta_2)) = 0$ *which corresponds to*

- $\theta_1 = 0$ *or* π, $\theta_2 = 0$ *or* π, $\theta_1 = \theta_2$.

It is formed by the boundary of the physical domain: $\theta_1, \theta_2 \in [0, \pi], \theta_1 \leq \theta_2$, *with respective controls* $(0, 1)$, $(1, 0)$, $(1, 1)$ *and the edges of the triangle are Martinet points. The associated adjoint vector is constant and can be normalized to* $p = (1, 0, 0)$. *Thus the triangle is a piecewise smooth abnormal stroke.*

Remark 3.1. The previous lemma provides the interpretation of the policy represented in Fig.3 which corresponds exactly to the abnormal stroke. Note it will form the boundary of the domain. A recent contribution[15] proves that such an abnormal curve with a corner cannot be optimal, not taking into account the state constraints. Our related analysis with the concept of efficiency will be interesting in the framework of SR-geometry.

3.2. *The normal case*

To analyze the first situation describes in Fig.2, the mechanical energy has to be used in relation with SR-geometry.

3.2.1. *Preliminaries*

For the SR-problem an orthonormal frame can be computed as follows. Using the following feedback transformation

$$\begin{pmatrix} u_1 \\ u_2 \end{pmatrix} = \begin{pmatrix} \cos(\alpha) & \sin(\alpha) \\ -\sin(\alpha) & \cos(\alpha) \end{pmatrix} \begin{pmatrix} v_1 \\ v_2 \end{pmatrix}$$

where $\alpha = \arctan\left(\frac{2\sin(\theta_1)\sin(\theta_2)}{\sin^2(\theta_2)-\sin^2(\theta_1)}\right) = \begin{cases} \arctan\left(\frac{\sin(\theta_1)}{\sin(\theta_2)}\right) & \text{if } \sin(\theta_1) \leq \sin(\theta_2) \\ -\arctan\left(\frac{\sin(\theta_2)}{\sin(\theta_1)}\right) & \text{if } \sin(\theta_1) > \sin(\theta_2) \end{cases}$,
the mechanical system takes the form:

$$\begin{cases} \delta_1 v_1^2 + \delta_2 v_2^2 & \text{if } \sin(\theta_1) \leq \sin(\theta_2) \\ \delta_2 v_1^2 + \delta_1 v_2^2 & \text{if } \sin(\theta_1) > \sin(\theta_2) \end{cases}$$

where $\delta_1 = \frac{1}{3}$, $\delta_2 = \frac{1}{6}\frac{4-\sin^2(\theta_1)-\sin^2(\theta_2)}{2+\sin^2(\theta_1)+\sin^2(\theta_2)}$.
Introducing

$$\begin{cases} w_1 = \delta_1 v_1,\ w_2 = \delta_2 v_2 & \text{if } \sin(\theta_1) \leq \sin(\theta_2) \\ w_1 = \delta_2 v_1,\ w_2 = \delta_1 v_2 & \text{if } \sin(\theta_1) > \sin(\theta_2) \end{cases}$$

the mechanical energy takes the form $w_1^2 + w_2^2$.

We shall not use this reduction to make our computations and we use directly the normal Hamiltonian associated to the metric $a(q)u_1^2 + 2b(q)u_1u_2 + c(q)u_2^2$ which

takes the form (with $\lambda_0 = -1/2$)

$$H_n(q,p) = \frac{1}{2}\left(a(q)u_1^2 + 2b(q)u_1u_2 + c(q)u_2^2\right). \tag{3.2}$$

where the optimal controls u_1, u_2 are computed with

$$\begin{cases} H_1(q,p) = a(q)u_1 + b(q)u_2, \\ H_2(q,p) = b(q)u_1 + c(q)u_2 \end{cases}$$

3.2.2. *Simplified cost*

Note that if the cost is simplified to $\int_0^T (u_1^2 + u_2^2)\mathrm{d}t$, some geometric computations can be made, in relation with the Heisenberg case and which can be used in the numerical implementation, in particular to compute strokes with small amplitudes. In this case,

$$H_n = \frac{1}{2}\left(H_1^2 + H_2^2\right)$$

and straightforward computations inside the abnormal triangle are the following using the Poincaré coordinates (q, H), $H = (H_1, H_2, H_3)$ and $H_i = p \cdot G_i(q)$. Indeed:

$$\dot{H}_1 = \mathrm{d}H_1(\vec{H_n}) = \{H_1, H_2\}H_2 = H_2H_3,$$
$$\dot{H}_2 = \mathrm{d}H_2(\vec{H_n}) = \{H_2, H_1\}H_1 = -H_1H_3,$$

Moreover

$$\dot{H}_3 = \mathrm{d}H_3(\vec{H_n}) = \{H_3, H_1\}H_1 + \{H_3, H_2\}H_2,$$

with

$$\{H_3, H_1\}(z) = p \cdot [[G_1, G_2], G_1](q)\{H_3, H_2\}(z) = p \cdot [[G_1, G_2], G_2](q)$$

At a contact point, G_1, G_2, G_3 form a frame, therefore

$$[[G_1, G_2], G_1](q) = \sum_{i=1}^{3} \lambda_i(q)G_i(q)$$

where moreover $\lambda_1 = \lambda_2 = 0$, $\frac{\partial f}{\partial \theta_1} = \lambda_3 f$.
Similarly,

$$[[G_1, G_2], G_2](q) = \sum_{i=1}^{3} \lambda_i'(q)G_i(q),$$

with

$$\lambda_1' = \lambda_2' = 0, \qquad \frac{\partial f}{\partial \theta_2} = \lambda_3' f.$$

We conclude that

$$\dot{H}_1 = H_2H_3, \quad \dot{H}_2 = -H_1H_3,$$
$$\dot{H}_3 = H_3\left(\lambda_3 H_1 + \lambda_3' H_2\right). \tag{3.3}$$

The associated one dimensional distribution can be analyzed setting $\mathrm{d}s = H_3\mathrm{d}t$ and we obtain

$$\frac{\mathrm{d}H_1}{\mathrm{d}s} = H_2, \qquad \frac{\mathrm{d}H_2}{\mathrm{d}s} = -H_1, \qquad \frac{\mathrm{d}H_3}{\mathrm{d}s} = \lambda_3 H_1 + \lambda_3' H_2.$$

In particular, we have the harmonic oscillator since $H_1'' + H_1 = 0$, differentiating with respect to s.
Furthermore H_3 can be analyzed using the remaining equation (3.3). Observe that with the approximation λ_3, λ_3' constant, the equation takes the form

$$\frac{\mathrm{d}H_3}{\mathrm{d}s} = A\cos(s+\rho).$$

with A, ρ constant. In those computations, we recognized the Heisenberg case, corresponding to $\lambda_3 = \lambda_3' = 0$.
Note that in order to deal with the Martinet case, one can choose the frame G_1, G_2 and $G_3 = \partial/\partial x$.

3.2.3. *Commented numerical results not taking into account the state constraints*

The objective of this section is to analyze the two following problems:

- **Problem 1:** From the micro-local point of view, variety of the different kind of normal strokes e.g. simple loop, eight, limaçon realizable normal strokes by the Copepod swimmer in relation with the classification of planar periodic curves, [4] see Fig.4.

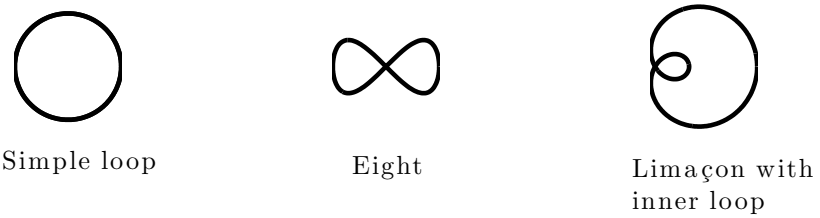

Fig. 4: Non equivalent strokes.

  For this study, we lift the angles $\theta_i \in S^1$ to the covering space $\mathbb{R}$.
- **Problem 2:** Compute the conjugate points along a normal stroke to select the candidates for optimality. Recall that[8,2] a normal stroke is C^1-optimal up to the first conjugate point.

Numerical methods The period T is fixed to 2π in our simulations. We use the `HamPath` software[14] at two levels:

(1) The shooting equations associated with the problem are

$$\begin{aligned} &x_0(0) = 0, && x_0(2\pi) = x_f, \\ &\theta_{1|2}(0) = \theta_{1|2}(2\pi), && p_{2|3}(0) = p_{2|3}(2\pi). \end{aligned}$$

(2) For a normal stroke given, testing its optimality by showing the nonexistence of conjugate points using the variational equation to compute Jacobi fields. Recall that[8] given a reference curve $(q(t), p(t))$ solution of $\overrightarrow{H_n}$, a time $t_c \in]0, 2\pi]$ is a conjugate time if there exists a Jacobi field $\delta z = (\delta q, \delta p)$, that is a non-zero solution of the variational equation

$$\dot{\delta z}(t) = \frac{\partial \vec{H}_n}{\partial z}(q(t), p(t))\delta z(t) \tag{3.4}$$

such that $\delta q(0) = \delta q(t_c) = 0$. We denote $\delta z_i = (\delta q_i, \delta p_i)$, $i = 1...n$, n-independent solutions of (3.4) with initial condition $\delta q(0) = 0$. At time t_c we have the following rank condition

$$\text{rank}\{\delta q_1(t_c), ..., \delta q_n(t_c)\} < n. \tag{3.5}$$

Complexity of optimal policies We present some simulations of normal strokes not taking into account the state constraints. Fig.5 illustrates three different strokes confirming the complexity of the model and are related to the generic classification of periodic planar curves,[4]. Conjugate points are also computed to check the second order optimality conditions. There is no conjugate points on $[0, 2\pi]$ in the case of the simple loop whereas they appear for the limaçon case, the eight case and more complicated cases. *Hence, the only candidates for optimality are the simple loops.*

3.2.4. *Optimal curves circumscribed in the triangle of constraints*

We use a combination of the `Bocop` and `HamPath` softwares.

- `Bocop` This software is suitable to take into account de state constraints on the shape variables. Fig.6 describes a single loop tangent to the boundary which is used to initialize the shooting algorithm of the `HamPath` software.
- `HamPath` This software cannot be directly applied to compute the optimal solution using the Maximum Principle with state constraints, due to the complexity of the different principles,[10].

Fixing the energy level $H_n = 1/2$, the domain of the exponential map is not compact (cylinder) and the shooting problem consisting in finding an initial adjoint vector is ill-conditioned when computing normal extremals near the abnormal extremal. Fig.7 stresses this fact by representing the norm of the initial adjoint vector $p = (p_1, p_2, p_3)$ for different displacements, showing that the exponential map is non proper.

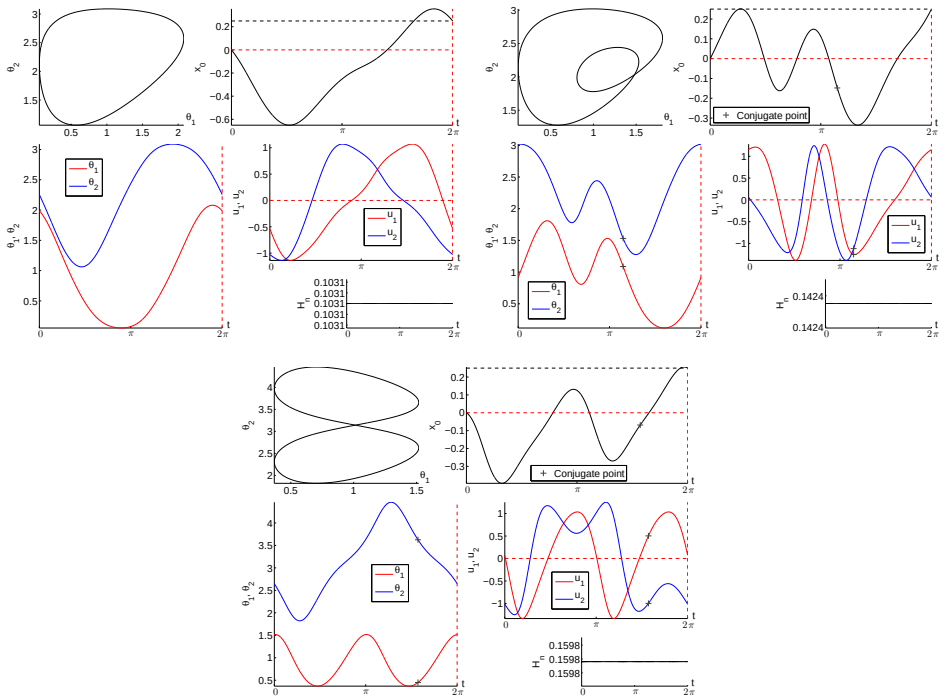

Fig. 5: Normal strokes : simple loop (left), limaçon with inner loop (right) and eight case (bottom). First conjugate points on $[0, 2\pi]$ appear with a cross only for the limaçon stroke and the eight stroke.

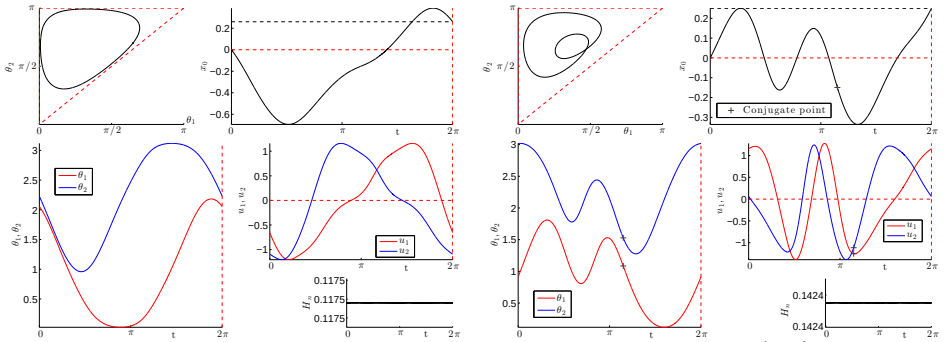

Fig. 6: Normal stroke where the constraints are satisfied: simple loop (left) and limaçon with inner loop (right).

Comparisons of the geometric efficiency of the strokes To compare the different normal and abnormal solutions corresponding to different displacements and in relation with the SR-interpretation we represent the ratio $\mathcal{E} = x_0/l$ where l is the length of the stroke and x_0 is the corresponding displacement (this quantity does not depend upon the parameterization).

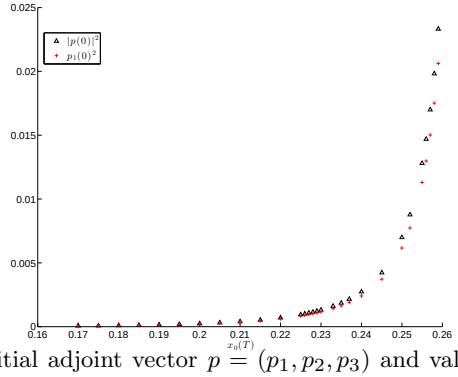

Fig. 7: Norm of the initial adjoint vector $p = (p_1, p_2, p_3)$ and value of $p_1(0)^2$ for normal strokes such that $H_n = 1/2$ and having different displacements, illustrating the non properness of the exponential mapping.

For the triangle, a displacement along the vertical or horizontal edge gives $x_0 = \frac{2\sqrt{3}}{3} \operatorname{arctanh}\left(\frac{\sqrt{3}}{3}\right)$ and along the hypotenuse $x_0 = -\sqrt{2} \operatorname{arctanh}\left(\frac{\sqrt{2}}{2}\right)$ and the total displacement is $2.742.10^{-1}$.
The length of a normal stroke γ is $l(\gamma) = \int_0^{2\pi} \sqrt{\dot{q} \cdot \dot{q}} \mathrm{d}t$ and is given by $2\pi\sqrt{2H_n}$ where H_n is the energy level. The efficiency curves are presented in Fig.8 where the normal strokes corresponding to the maximal efficiency is also represented.
Note that the geometric efficiency $\mathcal{E}$ is different from the concept of efficiency of the literature[13].

Application. From our analysis we deduce that the (triangle) abnormal stroke is not optimal. Indeed, one can choose a normal stroke (inside the triangle) such that the displacement is $\bar{x}_0/2$ with $\bar{x}_0 = 2.742$ and the length is less than $\bar{l}/2$ where $\bar{l}$ is the length of the triangle. Applying twice the normal stroke, we obtain the same displacement $\bar{x}_0$ than with the abnormal stroke but with a length $< \bar{l}$.

4. The Three-Link Purcell swimmer

4.1. *Symmetry properties*

First of all due to the structure of the equations (2.4) we have the following.

Lemma 4.1. *Let $\bar{q}(t) = (\bar{\theta}(t), \bar{x}(t), \bar{y}(t), \bar{\alpha}(t))$ and $q(t) = (\theta(t), x(t), y(t), \alpha(t))$ be the solutions associated with $u(.)$ with respective initial conditions $(\theta_0, 0, 0, 0)$ and $(\theta_0, 0, 0, \alpha_0)$ then*

$$\begin{aligned} &\bar{\theta}(t) = \theta(t), \quad \alpha(t) = \bar{\alpha}(t) + \alpha_0, \\ &x(t) = \cos(\alpha_0)\bar{x}(t) - \sin(\alpha_0)\bar{y}(t), \\ &y(t) = \sin(\alpha_0)\bar{x}(t) + \cos(\alpha_0)\bar{y}(t) \end{aligned} \tag{4.1}$$

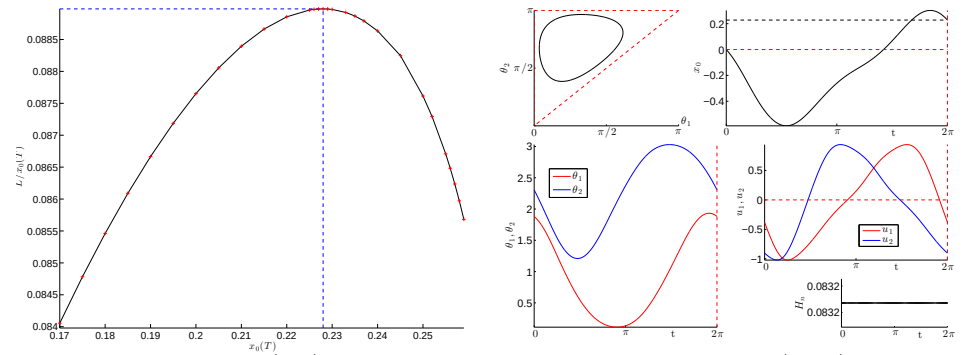

Fig. 8: Efficiency curve (left) and the corresponding minimizing curve (right). Note that the efficiency of the abnormal curve is $\mathbf{5.56e^{-2}}$ vs of order $\mathbf{8.60e^{-2}}$ for normal strokes.

Proof. We denote $A = \begin{pmatrix} 0 & -1 \\ 1 & 0 \end{pmatrix}$, $e^{At} = \begin{pmatrix} \cos(t) & -\sin(t) \\ \sin(t) & \cos(t) \end{pmatrix}$ and using (2.4), one has:

$$\frac{\mathrm{d}}{\mathrm{d}t}\begin{pmatrix} x(t) \\ y(t) \\ \alpha(t) \end{pmatrix} = \begin{pmatrix} \cos(\alpha) & -\sin(\alpha) & 0 \\ \sin(\alpha) & \cos(\alpha) & 0 \\ 0 & 0 & 1 \end{pmatrix}\begin{pmatrix} f_1(t) \\ f_2(t) \\ f_3(t) \end{pmatrix}$$

where $f_i(t)$, $i = 1 \dots 3$ are obtained integrating the θ-dynamics corresponding to $u(.)$ and with $\theta(0) = \theta_0$ and is independent of the (α, x, y)-variables.
One has

$$\alpha(t) = \int_0^t f_3(s)\mathrm{d}s + \alpha_0$$

and denoting $X = (x, y)^\intercal$, $\bar{X} = (\bar{x}, \bar{y})^\intercal$ and $V = (f_1, f_2)^\intercal$,

$$\begin{aligned} \frac{\mathrm{d}X}{\mathrm{d}t} &= e^{A\alpha(t)}V(t) \\ &= e^{A(\alpha_0 + \int_0^t f_3(s)\mathrm{d}s)}V(t) \\ &= e^{A\alpha_0}e^{A\int_0^t f_3(s)\mathrm{d}s}V(t) \\ &= e^{A\alpha_0}\frac{\mathrm{d}\bar{X}}{\mathrm{d}t} \end{aligned}$$

Hence, integrating, one gets the remaining equation (4.1) that is

$$X(t) = e^{A\alpha_0}\bar{X}(t). \qquad \square$$

Lemma 4.2. *Let H_n be the extremal normal Hamiltonian associated with any quadratic cost $\int_0^{2\pi}(a(q)u_1^2 + 2b(q)u_1u_2 + c(q)u_2^2)\mathrm{d}t$. Denoting $(p_\theta, p_x, p_y, p_\alpha)$ the adjoint components, we have the following first integrals*

$$I_1 = p_x,\ I_2 = p_y,\ I_3 = H_n,\ I_4 = (p_x y - p_y x) - p_\alpha$$

Proof. The proof results from straightforward computations. □

Corollary 4.1. *Consider the shooting conditions*

- θ, α 2π*-periodic,*
- $x(0) = y(0) = 0$,
- $(p_x y - x p_y)(2\pi) = 0$
- p_θ, p_α 2π*-periodic,*
- $(x^2 + y^2)(2\pi) = r^2$,
- $((p_x, p_y)(2\pi)$ *normal to* $S(r) : x^2 + y^2 = r^2)$.

Since $I_4 = (p_x y - x p_y) - p_\alpha$ is a first integral, at $t = 0$ and $t = 2\pi$ we have $p_x y - p_y x = 0$, then we deduce $p_\alpha(0) = p_\alpha(2\pi)$. Hence the assertion p_α is 2π-periodic is equivalent to p is normal to $S(r)$ and one of the conditions can be relaxed and be replaced by $\alpha(0) = 0$ to determine the solution.

4.2. *Nilpotent approximation*

Due to the mathematical complexity of the model, the nilpotent approximation will play a crucial role in our computations. First of all, thanks to the integrability of the associated normal extremals in the class of elliptic functions, it will allow to make a micro-local analysis of the different kind of strokes and to estimate the conjugate points using a proper time rescaling. Secondly, the abnormal extremals forming piecewise smooth strokes can be easily computed in this approximation and their optimality studied using the corresponding concept of conjugate point.

4.2.1. *The flat nilpotent model*

There is a unique nilpotent model associated with a 2-dimensional distribution with grow vector $(2, 3, 5)$ which is described next[12,27].

Definition 4.1. We call the flat Cartan model the 2-dimensional distribution in dimension five defined by the two vector fields:

$$\hat{F}_1(\hat{q}) = \frac{\partial}{\partial \hat{q}_1},\ \hat{F}_2(\hat{q}) = \frac{\partial}{\partial \hat{q}_2} + \hat{q}_1 \frac{\partial}{\partial \hat{q}_3} + \frac{\partial}{\partial \hat{q}_4} + \hat{q}_1^2 \frac{\partial}{\partial \hat{q}_5}.$$

where $\hat{q} = (\hat{q}_1, \hat{q}_2, \hat{q}_3, \hat{q}_4, \hat{q}_5)$ will be the privileged coordinates with the following weights: 1 for $\hat{q}_1, \hat{q}_2$, 2 for $\hat{q}_3$ and 3 for $\hat{q}_4, \hat{q}_5$.

4.2.2. *Computations of the nilpotent approximation*

The Purcell system (2.4) is written as $\dot{q} = Fu = \sum_{i=1}^{2} u_i F_i$ where the two vectors fields are explicitly given[22]. The nilpotent approximation is computed at $q_0 = 0$ and will provide a nilpotent approximation of the SR-problem for the simplified cost $\int_0^{2\pi} (u_1^2 + u_2^2) \mathrm{d}t$ which is sufficient in our theoretical analysis. Assuming $l = 2, l_1 = l_2 = 1$ and the standard normalization $c_t = 1, c_n = 2c_t$ of the respective

tangential and normal drag coefficients, the two-jets of F_1 and F_2 at zero are

$$\begin{aligned}
F_1(q) &= \frac{\partial}{\partial q_1} + \left(-\frac{1}{6}\,q_5 - \frac{4}{27}\,q_1 - \frac{2}{27}\,q_2\right)\frac{\partial}{\partial q_3} \\
&\quad + \left(\frac{1}{6} - \frac{1}{12}\,{q_5}^2 - \frac{2}{27}\,q_5\,q_2 - \frac{4}{27}\,q_5\,q_1 - \frac{1}{27}\,{q_1}^2 - \frac{1}{27}\,q_1 q_2 - \frac{1}{36}\,{q_2}^2\right)\frac{\partial}{\partial q_4} \\
&\quad + \left(-\frac{7}{27} + \frac{2}{81}\,{q_1}^2 - \frac{2}{81}\,q_1 q_2 - \frac{5}{162}\,{q_2}^2\right)\frac{\partial}{\partial q_5} + O(|q|^3) \\
F_2(q) &= \frac{\partial}{\partial q_2} + \left(\frac{1}{6}\,q_5 + \frac{4}{27}\,q_2 + \frac{2}{27}\,q_1\right)\frac{\partial}{\partial q_3} \\
&\quad + \left(-\frac{1}{6} + \frac{1}{12}\,{q_5}^2 + \frac{4}{27}\,q_5\,q_2 + \frac{2}{27}\,q_5\,q_1 + \frac{1}{36}\,{q_1}^2 + \frac{1}{27}\,q_1 q_2 + \frac{1}{27}\,{q_2}^2\right)\frac{\partial}{\partial q_4} \\
&\quad + \left(-\frac{7}{27} - \frac{5}{162}\,{q_1}^2 - \frac{2}{81}\,q_1 q_2 + \frac{2}{81}\,{q_2}^2\right)\frac{\partial}{\partial q_5} + O(|q|^3)
\end{aligned}$$

We compute the local diffeomorphism φ to reduce F_1, F_2 to the nilpotent approximation $\hat{F}_1, \hat{F}_2$ using the sequence $\varphi = \varphi_N \; o \; ... \; o \; \varphi_1 : \mathbb{R}^5 \to \mathbb{R}^5$ with $N = 13$ and φ_i are simple change of coordinates that we describe next.
At each step i, we denote $q = (q_1, q_2, q_3, q_4, q_5)$ the old local coordinates and $Q = (Q_1, Q_2, Q_3, Q_4, Q_5)$ the new ones: $q = \varphi_i(Q)$ and each φ_i has only one non trivial component, the other components being the identity transformation and are not specified.

(1) $q_5 = \varphi_1^{(5)}(Q_5) = Q_5 - \frac{7}{27}Q_1$,
(2) $q_3 = \varphi_2^{(3)}(Q_3) = Q_3 - \frac{1}{6}Q_5Q_1 - \frac{17}{324}Q_1^2 - \frac{2}{27}Q_2Q_1$,
(3) $q_4 = \varphi_3^{(4)}(Q_4) = Q_4 + \frac{1}{6}Q_1 - \frac{37}{26244}Q_1^3$,
(4) $q_5 = \varphi_4^{(5)}(Q_5) = Q_5 + \frac{2}{24}Q_1^3 - \frac{2}{162}$,
(5) $q_5 = \varphi_5^{(5)}(Q_5) = Q_5 - \frac{7}{27}Q_2$,
(6) $q_3 = \varphi_6^{(3)}(Q_3) = \frac{5}{81}Q_3 + \frac{17}{324}Q_2^2 + \frac{1}{6}Q_5Q_2$,
(7) $q_4 = \varphi_7^{(4)}(Q_4) = Q_4 - Q_3Q_2$,
(8) $q_4 = \varphi_8^{(4)}(Q_4) = Q_4 + \frac{37}{26244}Q_2^3$,
(9) $q_4 = \varphi_9^{(4)}(Q_4) = Q_4 - \frac{4482}{8748}Q_5$,
(10) $q_4 = \varphi_{10}^{(4)}(Q_4) = Q_4 + \frac{2270}{2187}Q_2Q_3 + \frac{5}{81}Q_5Q_3 + \frac{83}{19683}Q_2^3$,
(11) $q_4 = \varphi_{11}^{(4)}(Q_4) = -\frac{83}{2187}Q_4$,
(12) $q_5 = \varphi_{12}^{(5)}(Q_5) = Q_5 + \frac{1}{27}Q_3Q_2 + \frac{2}{243}Q_2^3$,
(13) $q_5 = \varphi_{13}^{(5)}(Q_5) = -\frac{1}{54}Q_5 - \frac{1}{27}Q_4$.

This leads to a complicated transformation whose role is to relate the privileged coordinates to the physical coordinates $(\theta_1, \theta_2, x, y, \alpha)$ in particular we have:

Lemma 4.3. *The shape variables $\theta = (\theta_1, \theta_2)$ corresponds to the $(\hat{q}_1, \hat{q}_2)$ coordinates.*

4.2.3. *Integration of normal extremal trajectories*

Computing with (4.1), one has

$$\hat{F}_1(\hat{q}) = \frac{\partial}{\partial \hat{q}_1}, \qquad \hat{F}_2(\hat{q}) = \frac{\partial}{\partial \hat{q}_2} + \hat{q}_1 \frac{\partial}{\partial \hat{q}_3} + \hat{q}_3 \frac{\partial}{\partial \hat{q}_4} + \hat{q}_1^2 \frac{\partial}{\partial \hat{q}_5},$$
$$[\hat{F}_1, \hat{F}_2](\hat{q}) = -\frac{\partial}{\partial \hat{q}_3} - 2\hat{q}_1 \frac{\partial}{\partial \hat{q}_5}, \quad [[\hat{F}_1, \hat{F}_2], \hat{F}_1](\hat{q}) = -2\frac{\partial}{\partial \hat{q}_5},$$
$$[[\hat{F}_1, \hat{F}_2], \hat{F}_2](\hat{q}) = \frac{\partial}{\partial \hat{q}_4}.$$

All brackets of length greater than 3 are zero.
Introducing the hamiltonian lifts, one has:

$$H_1(\hat{z}) = \langle \hat{p}, \hat{F}_1(\hat{q}) \rangle = \hat{p}_1, \qquad H_2(\hat{z}) = \langle \hat{p}, \hat{F}_2(\hat{q}) \rangle = \hat{p}_2 + \hat{p}_3\hat{q}_1 + \hat{p}_4\hat{q}_3 + \hat{p}_5\hat{q}_1^2,$$
$$H_3(\hat{z}) = \langle \hat{p}, [\hat{F}_1, \hat{F}_2](\hat{q}) \rangle = -\hat{p}_3 - 2\hat{q}_1\hat{p}_5, \quad H_4(\hat{z}) = \langle \hat{p}, [[\hat{F}_1, \hat{F}_2], \hat{F}_1](\hat{q}) \rangle = -2\hat{p}_5,$$
$$H_5(\hat{z}) = \langle \hat{p}, [[\hat{F}_1, \hat{F}_2], \hat{F}_2](\hat{q}) \rangle = \hat{p}_4.$$

The SR-Cartan flat case is

$$\dot{\hat{q}} = \sum_{i=1}^{2} u_i \hat{F}_i, \quad \min_u \int_0^{2\pi} (u_1^2 + u_2^2) \mathrm{d}t.$$

and the normal Hamiltonian takes the form

$$H_n = \frac{1}{2}(H_1^2 + H_2^2) \tag{4.2}$$

or, more precisely the system is written

$$\begin{aligned} &\dot{\hat{q}}_1 = H_1, \qquad \dot{\hat{q}}_2 = H_2, \qquad \dot{\hat{q}}_3 = H_2\hat{q}_1, \\ &\dot{\hat{q}}_4 = H_2\hat{q}_3, \qquad \dot{\hat{q}}_5 = H_2\hat{q}_1^2. \end{aligned} \tag{4.3}$$

Computing we have

$$\dot{H}_1 = \mathrm{d}H_1(\vec{H}) = \{H_1, H_2\}H_2 = \langle \hat{p}, [\hat{F}_1, \hat{F}_2](\hat{q}) \rangle H_2 = H_2H_3,$$
$$\dot{H}_2 = -H_3H_1, \qquad \dot{H}_3 = H_1H_4 + H_2H_5,$$
$$\dot{H}_4 = 0 \quad \text{hence} \quad H_4 = c_4, \quad \dot{H}_5 = 0 \quad \text{hence} \quad H_5 = c_5.$$

Fixing the level energy, $H_1^2 + H_2^2 = 1$ we set $H_1 = \cos(\theta)$ and $H_2 = \sin(\theta)$.

$$\dot{H}_1 = -\sin(\theta)\dot{\theta} = H_2H_3 = \sin(\theta)H_3.$$

Hence $\dot{\theta} = -H_3$ and

$$\ddot{\theta} = -(H_1c_4 + H_2c_5) = -c_4\cos(\theta) - c_5\sin(\theta) = -\omega^2\sin(\theta + \phi)$$

where ω and ϕ are constant. More precisely, we have

$$\omega = \left(\hat{p}_4(0)^2 + 4\hat{p}_5(0)^2\right)^{1/4}, \quad \phi = \arctan\left(\frac{-2\,\hat{p}_5(0)}{\hat{p}_4(0)}\right).$$

Let $\psi = \theta + \phi$, we get

$$\frac{1}{2}\dot{\psi}^2 - \omega^2 \cos(\psi) = B, \tag{4.4}$$

where B is a constant

$$B = 1/2\ (\hat{p}_3(0) + 2\,\hat{q}_1(0)\hat{p}_5(0))^2 - \hat{p}_1(0)\,\hat{p}_4(0) - 2\,\hat{p}_5(0)\,\hat{p}_2(0) - 2\,\hat{p}_5(0)\,\hat{p}_4(0)\,\hat{x}_3(0).$$

We distinguish the two following cases.

- *Oscillating case.* We introduce $k^2 = \frac{1}{2} + \frac{B}{2\omega^2}$ with $0 < k < 1$ so that (4.4) becomes

$$\dot{\psi}^2 = 4\omega^2 \left(k^2 - \sin^2(\frac{\psi}{2})\right)$$

and we obtain[18]

$$\sin(\psi/2) = k\,\mathrm{sn}(u,k), \quad \cos(\psi/2) = \mathrm{dn}(u,k)$$

where $u = \omega t + \varphi_0$.
H_1 and H_2 are elliptic functions of the first kind and $\hat{q}_1, \hat{q}_2$, solutions of (4.3), are expressed as

$$\begin{aligned} \hat{q}_1(u) &= \hat{q}_{10} + \frac{1}{\omega}\Big[-2\,k\,\sin(\phi)\,\mathrm{cn}(u) + (-u + 2\,E(u))\cos(\phi)\Big] \\ \hat{q}_2(u) &= \hat{q}_{20} + \frac{1}{\omega}\Big[-2\,k\,\cos(\phi)\,\mathrm{cn}(u) + (u - 2\,E(u))\sin(\phi)\Big] \end{aligned} \tag{4.5}$$

where $\hat{q}_{10}, \hat{q}_{20}$ are constant.
- *Rotating case.* We introduce $k^2 = \frac{2\omega^2}{B+\omega^2}$ with $0 < k < 1$ so that (4.4) becomes

$$\dot{\psi}^2 = \frac{4\omega^2}{k^2}\left(1 - k^2\sin^2(\frac{\psi}{2})\right).$$

and we obtain[18]

$$\sin(\psi/2) = \mathrm{sn}(\frac{u}{k},k), \quad \cos(\psi/2) = \mathrm{cn}(\frac{u}{k},k)$$

where $u = \omega t + \varphi_0$.
H_1 and H_2 are elliptic functions of the first kind and $\hat{q}_1, \hat{q}_2$ solutions of (4.3) are expressed as

$$\begin{aligned}\hat{q}_1(u) = \hat{q}_{10} + \frac{1}{\omega}\Bigg[&\Big(1 - \frac{2}{k^2} + 2\,\frac{\mathrm{E}\,(k)}{k^2\,\mathrm{K}\,(k)}\Big)\cos(\phi)\,u \\ &+ \frac{2}{k}\left(\cos(\phi)\,\mathrm{Z}\left(\frac{u}{k}\right) - \sin(\phi)\,\mathrm{dn}\left(\frac{u}{k}\right)\right)\Bigg] \\ \hat{q}_2(u) = \hat{q}_{20} + \frac{1}{\omega}\Bigg[&\Big(\frac{2}{k^2} - 1 - 2\,\frac{\mathrm{E}\,(k)}{k^2\,\mathrm{K}\,(k)}\Big)\sin(\phi)\,u \\ &- \frac{2}{k}\left(\sin(\phi)\,\mathrm{Z}\left(\frac{u}{k}\right) + \cos(\phi)\,\mathrm{dn}\left(\frac{u}{k}\right)\right)\Bigg]\end{aligned} \tag{4.6}$$

where $\hat{q}_{10}, \hat{q}_{20}$ are constant.

4.2.4. *Computations of strokes with small amplitudes using the nilpotent approximation*

We recall that the physical variables q are related to $\hat{q}$ using the transformation φ. The adjoint variables p are obtained by a Mathieu transformation associated with φ. Strokes with small amplitudes such that $q(0) = 0$ are computed from the nilpotent approximation in the following ways:

- *Oscillating case:*
  The modulus k can be expressed as
  $$k(\hat{p}(0)) = \frac{1}{2}\sqrt{\frac{2\sqrt{\hat{p}_4(0)^2 + 4\,\hat{p}_5(0)^2} + \hat{p}_3(0)^2 - 2\,\hat{p}_1(0)\,\hat{p}_4(0) - 4\,\hat{p}_5(0)\,\hat{p}_2(0)}{\sqrt{\hat{p}_4(0)^2 + 4\,\hat{p}_5(0)^2}}} \tag{4.7}$$
  and computing $k(\hat{p}(0)) = k_p$ such that the linear terms of $\theta_1(t) = \hat{q}_1(\omega t + \varphi_0), \theta_2(t) = \hat{q}_2(\omega t + \varphi_0)$ of (4.5) vanish leads to periodic strokes with eight shapes of period
  $$T = \frac{4\,K(k)}{\left(\hat{p}_4(0)^2 + 4\,\hat{p}_5(0)^2\right)^{1/4}}.$$
  The constant $\hat{q}_{10}, \hat{q}_{20}$ are chosen such that $\theta(0) = 0$. The initial adjoint vector $p(0)$ has to check the conditions $H_1(\hat{q}(0), \hat{p}(0))^2 + H_2(\hat{q}(0), \hat{p}(0))^2 = 1$, $k(\hat{p}(0)) = k_p \in (0, 1)$ and $\hat{p}_4(0)^2 + 4\,\hat{p}_5(0)^2 \neq 0$. We integrate numerically the stroke in the physical variables starting from $(q(0) = 0, p(0))$ and compute the first conjugate points on $[0, T]$ (see Fig.9).
- *Rotating case:* The modulus k can be expressed as
  $$k(\hat{p}(0)) = 2\sqrt{\frac{\sqrt{\hat{p}_4(0)^2 + 4\,\hat{p}_5(0)^2}}{2\sqrt{\hat{p}_4(0)^2 + 4\,\hat{p}_5(0)^2} + \hat{p}_3(0)^2 - 2\,\hat{p}_1(0)\,\hat{p}_4(0) - 4\,\hat{p}_5(0)\,\hat{p}_2(0)}} \tag{4.8}$$

We have $\theta_1(t) = \hat{q}_1(\omega t + \varphi_0), \theta_2(t) = \hat{q}_2(\omega t + \varphi_0)$ where $\hat{q}_1, \hat{q}_2$ are explicitly written in (4.6). We choose $p(0)$ so that $H_1(\hat{q}(0), \hat{p}(0))^2 + H_2(\hat{q}(0), \hat{p}(0))^2 = 1$, $k(\hat{p}(0)) \in (0, 1)$ and such that the denominator of $k(\hat{p}(0))$ is nonzero.
As $k(\hat{p}(0))$ tends to 0, the linear terms of $\hat{q}_1(u), \hat{q}_2(u)$ of (4.6) tend to 0 (see Fig.10). This is the case when $\hat{p}_4(0) \to 0$ and $\hat{p}_5(0) \to 0$, and the equation (4.4) becomes

$$\dot{\theta}^2 = \hat{p}_3(0)^2, \tag{4.9}$$

hence $\ddot{\theta} = 0$ and this case is treated below as the degenerated case.

- *Degenerated case:* We have

$$\ddot{\theta} = 0, \quad \dot{\theta}^2 = \hat{p}_3(0)^2,$$

hence $\theta(t) = \pm\hat{p}_3(0)\, t + \theta_0$ where θ_0 is a constant and the strokes are given by

$$\hat{q}_1(t) = \hat{q}_{10} + \frac{1}{\pm\hat{p}_3(0)} \sin(\pm\hat{p}_3(0)\, t + \theta_0),\ \hat{q}_2(t) = \hat{q}_{20} - \frac{1}{\pm\hat{p}_3(0)} \cos(\pm\hat{p}_3(0)\, t + \theta_0).$$

The constant $\hat{q}_{10}, \hat{q}_{20}$ are chosen such that $\theta(0) = 0$.
We integrate numerically the stroke in the physical variables starting from $(q(0) = 0, p(0))$ and compute the first conjugate points on $[0, T]$ (see Fig.11).

Abnormal case. We consider the minimal time problem for the single-input affine system[7]

$$\dot{\hat{q}}(t) = \hat{F}_1(\hat{q}(t)) + u(t)\hat{F}_2(\hat{q}(t))$$

where u is a scalar control.
Denoting $\hat{q}(.)$ a reference minimum time trajectory, since we consider abnormal extremals, it follows from the Pontryagin maximum principle that along the extremal lift of $\hat{q}(.)$, there must hold $H_2(\hat{q}(.), \hat{p}(.)) = 0$ and derivating with respect to t, $\{H_1, H_2\}(\hat{q}(.), \hat{p}(.)) = 0$ must hold too. Thanks to a further derivation, the extremals associated with the controls

$$u_a(\hat{q}, \hat{p}) = \frac{\{H_1, \{H_2, H_1\}\}(\hat{q}, \hat{p})}{\{H_2, \{H_1, H_2\}\}(\hat{q}, \hat{p})} = \frac{2\hat{p}_5}{\hat{p}_4}$$

satisfy the constraints $H_2 = \{H_1, H_2\} = 0$ along $(\hat{q}(.), \hat{p}(.))$ and are solutions of

$$\dot{\hat{q}} = \frac{\partial H_a}{\partial \hat{p}}, \quad \dot{\hat{p}} = -\frac{\partial H_a}{\partial \hat{q}}$$

where H_a is the true Hamiltonian

$$H_a(\hat{q}, \hat{p}) = H_1(\hat{q}, \hat{p}) + u_a H_2(\hat{q}, \hat{p}) = \hat{p}_1 + 2\, \frac{\hat{p}_5\, \left(\hat{p}_2 + \hat{p}_3\, \hat{q}_1 + \hat{p}_4\, \hat{q}_3 + \hat{p}_5\, \hat{q}_1^2\right)}{\hat{p}_4}.$$

From the Pontryagin maximum principle, the constraint $H_1(\hat{q}(.), \hat{p}(.)) = 0$ must hold too. The extremal system subject to the constraints $H_1 = H_2 = \{H_1, H_2\} = 0$

is integrable and solutions can be written as

$$\hat{q}_1(t) = t + \hat{q}_1(0), \qquad \hat{q}_2(t) = 2\,\frac{\hat{p}_5(0)\,t}{\hat{p}_4(0)} + \hat{q}_2(0),$$

$$\hat{q}_3(t) = \frac{\hat{p}_5(0)\,t^2}{\hat{p}_4(0)} + 2\,\frac{\hat{p}_5(0)\,\hat{q}_1(0)\,t}{\hat{p}_4(0)} + \hat{q}_3(0),$$

$$\hat{q}_4(t) = 2/3\,\frac{\hat{p}_5(0)^2 t^3}{\hat{p}_4(0)^2} - 2\,\frac{\hat{p}_5(0)\,\left(\hat{p}_5(0)\,\hat{q}_1(0)^2 + \hat{p}_3(0)\,\hat{q}_1(0) + \hat{p}_2(0)\right)t}{\hat{p}_4(0)^2}$$
$$- \frac{\hat{p}_5(0)\,\hat{p}_3(0)\,t^2}{\hat{p}_4(0)^2} + \hat{q}_4(0),$$

$$\hat{q}_5(t) = 2/3\,\frac{\hat{p}_5(0)\,t^3}{\hat{p}_4(0)} + \frac{(4\,\hat{p}_5(0)\,\hat{q}_1(0) + \hat{p}_3(0))\,t^2}{\hat{p}_4(0)}$$
$$+ 2\,\frac{\left(2\,\hat{p}_5(0)\,\hat{q}_1(0)^2 + \hat{p}_3(0)\,\hat{q}_1(0) + \hat{q}_3(0)\,\hat{p}_4(0) + \hat{p}_2(0)\right)t}{\hat{p}_4(0)} + \hat{q}_5(0),$$

$$\hat{p}_1(t) = \left(-2\,\frac{\hat{p}_5(0)\,\hat{p}_3(0)}{\hat{p}_4(0)} - 4\,\frac{\hat{p}_5(0)^2\hat{q}_1(0)}{\hat{p}_4(0)}\right)t + \hat{p}_1(0),$$

$$\hat{p}_2(t) = \hat{p}_2(0), \qquad \hat{p}_3(t) = -2\,\hat{p}_5(0)\,t + \hat{p}_3(0), \qquad \hat{p}_4(t) = \hat{p}_4(0), \qquad \hat{p}_5(t) = \hat{p}_5(0)$$

with $(\hat{q}_1(0), \hat{q}_2(0), \hat{q}_3(0), \hat{q}_4(0), \hat{q}_5(0), \hat{p}_1(0), \hat{p}_2(0), \hat{p}_3(0), \hat{p}_4(0), \hat{p}_5(0))$ are constant satisfying

$$\hat{p}_1(0) = 0,\ \hat{p}_2(0) = \hat{p}_5(0)\hat{q}_1(0)^2 - \hat{p}_4(0)\hat{q}_3(0),\ \hat{p}_3(0) = -2\hat{p}_5(0)\hat{q}_1(0).$$

Remark 4.1. The θ-projection abnormals are straight lines and will form triangles strokes.

4.3. *Commented numerical results*

4.3.1. *Computations of conjugate points*

Normal case. In the normal case, we consider the extremal system given by the true Hamiltonian given by (4.2). In section 4.2.3, we described three types of extremals computed with `HamPath`, and show the control, state and adjoint variables as functions of time (see Fig.11, Fig.9, Fig.10). We also illustrate the conjugate points computed according to the algorithm[10], as well as the smallest singular value for the rank test.

Property on the first conjugate point. For the normal extremals in the oscillating case and the rotating case presented in section 4.2.3, we take a large number of random initial adjoint vectors $\hat{p}(0)$ such that $H_1(\hat{q}(0), \hat{p}(0))^2 + H_2(\hat{q}(0), \hat{p}(0))^2 = 1$ and such that $0 < k(\hat{p}(0)) < 1$ where k is given by (4.7) for the oscillating case and by (4.8) for the rotating case. Then we numerically integrate the extremal system.

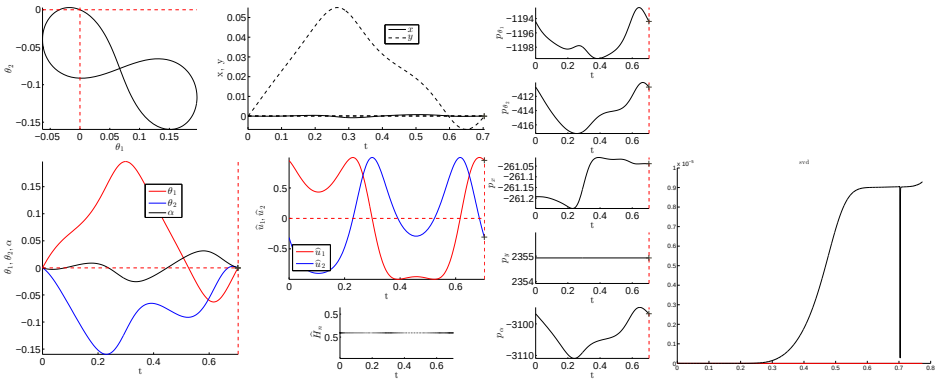

Fig. 9: *(left)* Control, state and adjoint physical variables in the oscillating case of the nilpotent approximation with an eight shape. *(right)* SVD test of conjugate points (the cross stands for the first conjugate point).

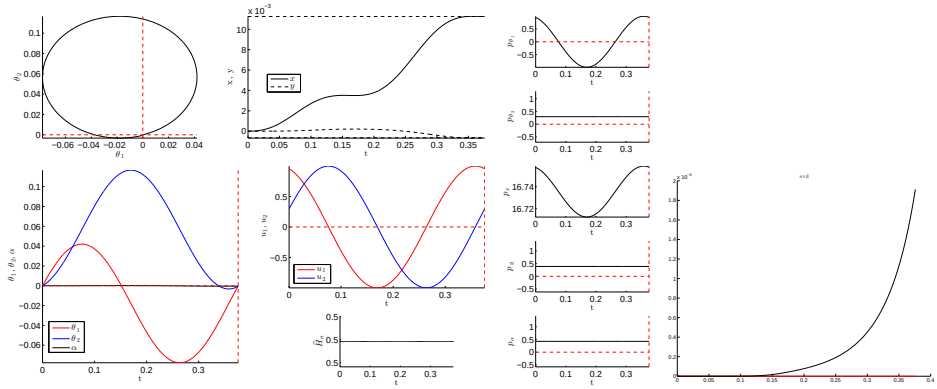

Fig. 10: *(left)* Control, state and adjoint physical variables in the rotating case of the nilpotent approximation ($k = 0.115$). *(right)* SVD test of conjugate points.

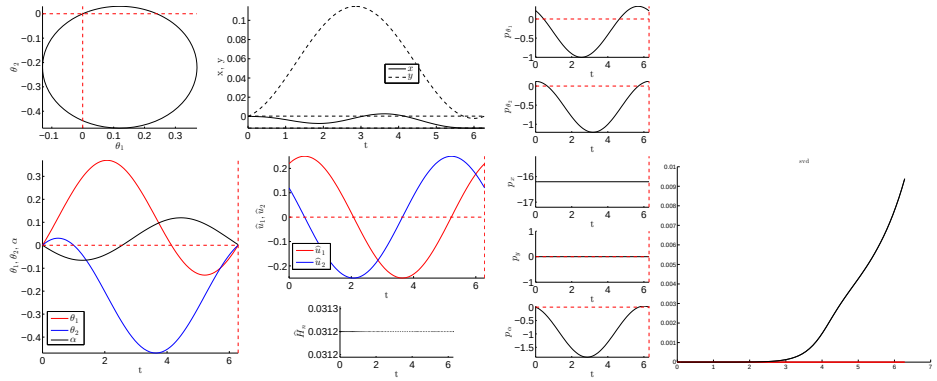

Fig. 11: *(left)* Control, state and adjoint physical variables in the degenerated case of the nilpotent approximation with an simple loop. *(right)* SVD test of conjugate points (no conjugate point on $[0, 2\pi]$).

We compute the first conjugate time t_{1c}, the pulsation $\omega = (\hat{p}_4(0)^2 + 4\,\hat{p}_5(0)^2)^{1/4}$, and the complete elliptic integral $K(k)$, where k is the modulus given by (4.7) in the oscillating case or by (4.8) in the rotating case.

Let $\gamma(.)$ be a normal extremal starting at $t = 0$ from the origin and defined on $[0, +\infty[$. As illustrated on Fig.12, there exist a first conjugate point along γ corresponding to a conjugate time t_{1c} satisfying the inequalities:

$$0.34\,\omega\,t_{1c} - 0.4 < K(k) < 0.53\,\omega\,t_{1c} - 0.8 \text{ for the oscillating case,}$$
$$0.33\,\omega\,t_{1c} + 0.16 < K(k) < 0.55\,\omega\,t_{1c} - 1.27 \text{ for the rotating case.}$$

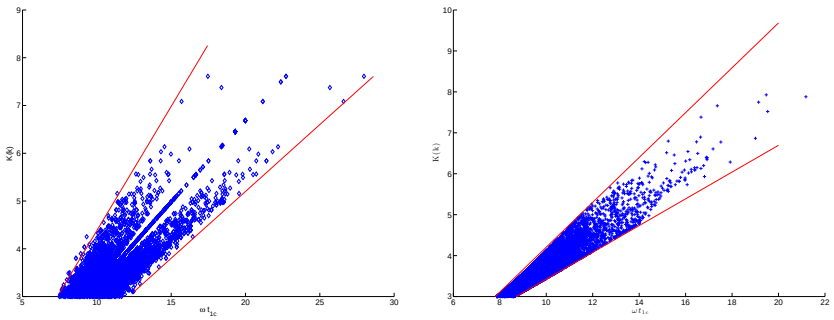

Fig. 12: Conjugate points of normal extremals with constant energy $H_1^2 + H_2^2 = 1$ in the oscillating case *(left)* and in the rotating case *(right)*.

Abnormal case. Fig.13 illustrates the time evolution of the state variables. We check numerically the second order optimality conditions[7]. The determinant test and smallest singular value for the rank condition both indicate that there is no conjugate time for abnormal extremals (Fig.14).

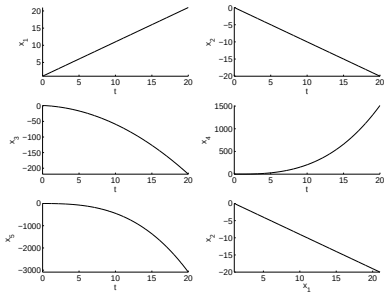

Fig. 13: Abnormal case: state variables for $\hat{q}(0) = (1, 0, 1, 0, 0)$, $\hat{p}(0) = (0, 0, -2, 1, 1)$.

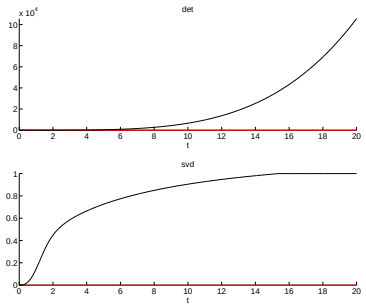

Fig. 14: Abnormal case: the second order sufficient condition indicates there is no conjugate point.

4.3.2. *Computations of optimal strokes using a discrete numerical homotopy*

Method

- The analytical expressions of $\theta_1(t), \theta_2(t)$ given in the degenerated case and in the oscillating case presented in section 4.2.3 allow us to compute strokes with small amplitudes of the nilpotent model. Besides, SVD test for conjugate points is also illustrated (see Fig.11 and Fig.9) showing that the simple loop have no conjugate points on $[0, T]$ while the eight stroke have a first conjugate point on $[0, T]$.
- The previous solutions are used to compute strokes for the Purcell swimmer with the $\int_0^T (u_1^2 + u_2^2)\mathrm{d}t$ cost. More precisely, the initial adjoint vector $\hat{p}(0)$ of the nilpotent model gives a good initialization of the shooting algorithm used by `HamPath` to solve the following boundary value problem.

$$\begin{cases} \dot{q} = \frac{\partial H_n}{\partial p}, \quad \dot{p} = -\frac{\partial H_n}{\partial q}, \\ \theta_{1|2}(T) = \theta_{1|2}(0), \\ x(0) = y(0) = \alpha(0) = 0, \\ x(T)^2 + y(T)^2 = c_1,\ \alpha(T) = c_2, \\ p_{\theta_{1|2}}(T) = p_{\theta_{1|2}}(0), p_\alpha(0) = p_\alpha(T) \end{cases} \tag{4.10}$$

where T, c_1, c_2 are fixed constants and H_n is the normal Hamiltonian associated with the $\int_0^T (u_1^2 + u_2^2)\mathrm{d}t$ cost.
Then, with T fixed to 2π and c_2 to 0, we perform a discrete homotopy on the radius c_1 to obtain stroke with larger amplitudes (see Fig.15).

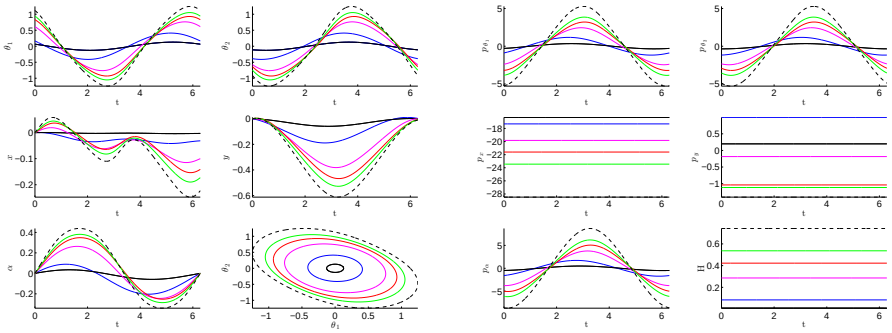

Fig. 15: One parameter family of simple loop strokes of the Purcell swimmer with the $\int_0^T (u_1^2 + u_2^2)\mathrm{d}t$ cost. The continuation is performed on the constant c_1 where we fixed $T = 2\pi$ and $c_2 = 0$.

Fig.16 (resp. Fig.17) illustrates state and adjoint variables for a simple loop stroke (resp. eight stroke) solution of (4.10) and it is obtained from $\hat{p}(0)$ given by the degenerated case (resp. oscillating case). There is no conjugate points on $[0, 2\pi]$ for the simple loop case while it appears for the eight case.

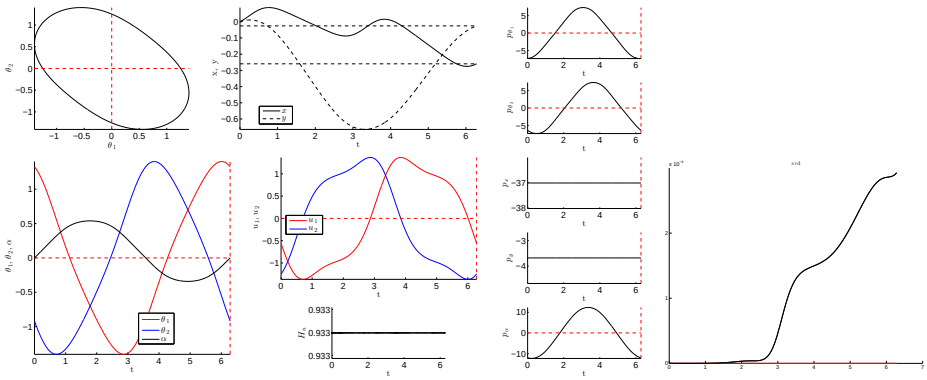

Fig. 16: *(left)* Simple loop stroke for the Purcell swimmer for the $\int_0^T (u_1^2 + u_2^2)\mathrm{d}t$ cost with $T = 2\pi$, $c_1 = 0.068$, $c_2 = 0$ and imposing the periodicity on α. *(right)* Test of conjugate points (no conjugate point on $[0, 2\pi]$).

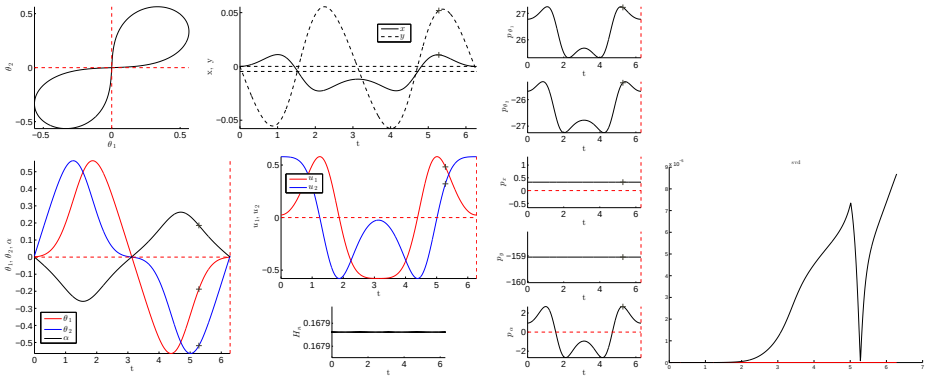

Fig. 17: *(left)* Eight stroke for the Purcell swimmer for the $\int_0^T (u_1^2+u_2^2)\mathrm{d}t$ cost with $T = 2\pi$, $c_1 = 4.6e{-}4$, $c_2 = 0$ and imposing the periodicity on α. *(right)* Test of conjugate points (the cross stands for the first conjugate point).

- Taking a solution of (4.10), we perform a discrete homotopy on the true Hamiltonian H_n associated with the $\int_0^T (u_1^2 + u_2^2)\mathrm{d}t$ cost to the Hamiltonian associated to the mechanical cost. We obtain a solution of the following boundary value problem, that is a stroke of the Purcell swimmer with the mechanical cost.

$$\begin{cases} \dot{q} = \frac{\partial H_n}{\partial p}, \quad \dot{p} = -\frac{\partial H_n}{\partial q}, \\ \theta_{1|2}(T) = \theta_{1|2}(0), \\ x(0) = y(0) = \alpha(0) = 0, \\ x(T)^2 + y(T)^2 = c_1,\ \alpha(T) = c_2, \\ p_{\theta_{1|2}}(T) = p_{\theta_{1|2}}(0), p_\alpha(0) = p_\alpha(T) \end{cases} \tag{4.11}$$

where $H = \frac{1}{2}\left(a(q)u_1^2 + 2b(q)u_1u_2 + c(q)u_2^2\right)$ is the true Hamiltonian associated to the mechanical cost and u_1, u_2 are the optimal controls.

Since the latter homotopy is discrete, we may not follow a unique branch and obtain many kind of strokes: Fig.18, Fig.19 and Fig.20 are three different strokes solutions of (4.11) and the SVD rank condition show that the only candidates for optimality are the simple loops.

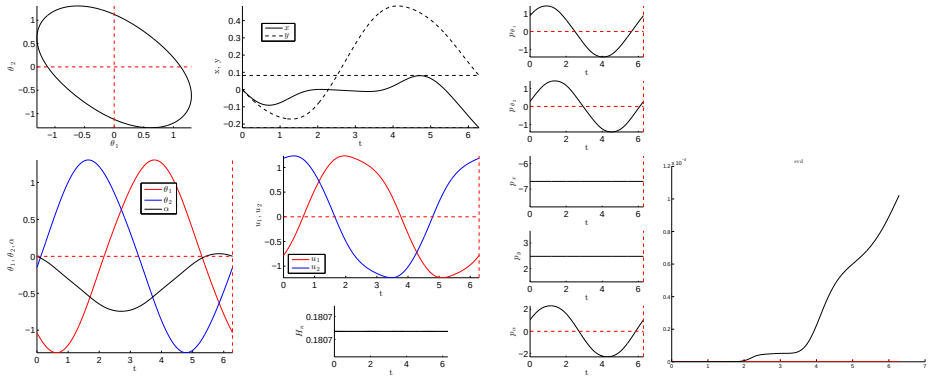

Fig. 18: *(left)* State and adjoint variables for the Purcell swimmer for the mechanical cost with $T = 2\pi$, $c_1 = 0.058$ and $c_2 = 0$. *(right)* Test of conjugate points (no conjugate point on $[0, 2\pi]$).

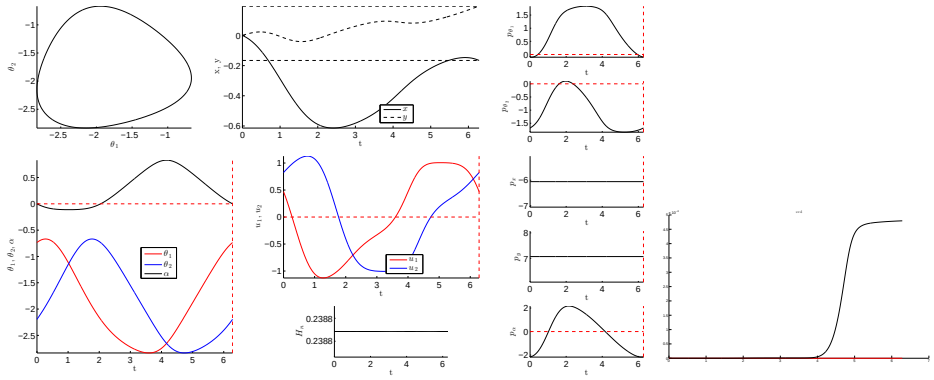

Fig. 19: *(left)* State and adjoint variables for the Purcell swimmer for the mechanical cost with $T = 2\pi$, $c_1 = 0.065$ and $c_2 = 0$. *(right)* Test of conjugate points (no conjugate point on $[0, 2\pi]$).

Then we perform a second homotopy on the radius c_1 to have a one-parameter family of strokes. Fig.21 and Fig.22 are two one-parameter families of solutions of (4.11) corresponding respectively to the strokes of Fig.18 and Fig.19.

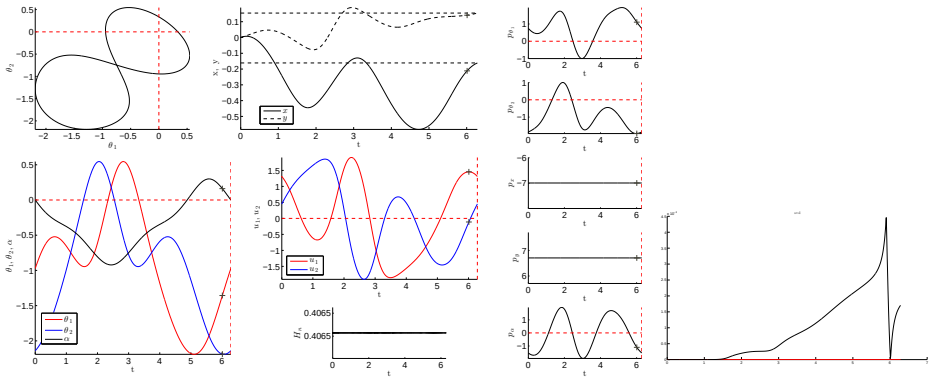

Fig. 20: *(left)* State and adjoint variables for the Purcell swimmer for the mechanical cost with $T = 2\pi$, $c_1 = 0.05$ and $c_2 = 0$. *(right)* Test of conjugate points (the cross stands for the first conjugate point).

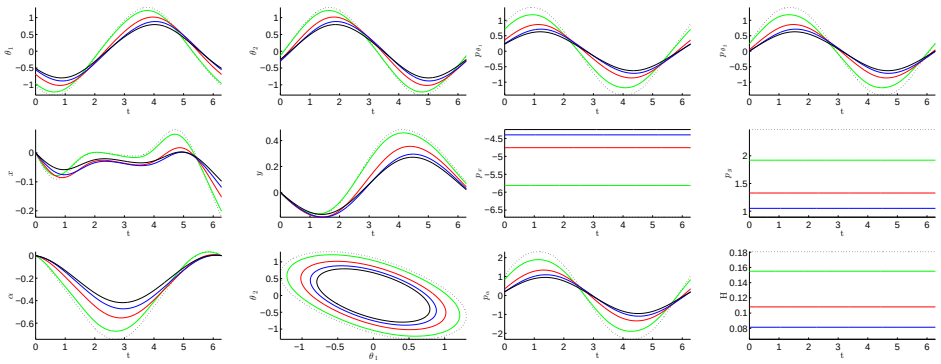

Fig. 21: Family 1 of strokes for the Purcell swimmer with the mechanical cost. We fixed $T = 2\pi$ and $c_2 = 0$ and the family of strokes is obtained by a continuation on c_1.

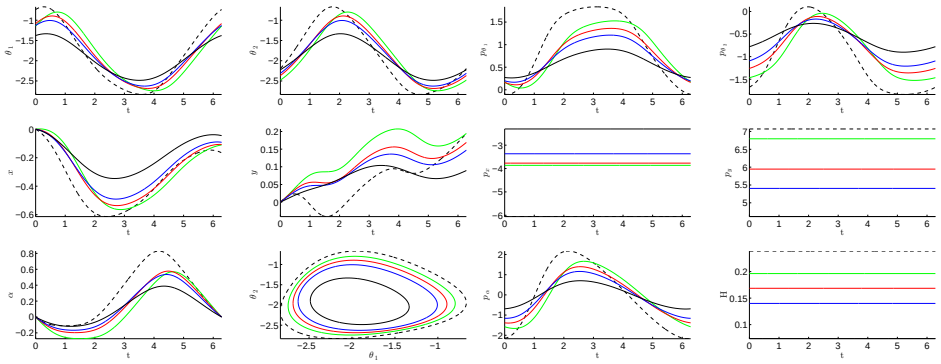

Fig. 22: Family 2 of strokes for the Purcell swimmer with the mechanical cost. We fixed $T = 2\pi$ and $c_2 = 0$ and the family of strokes is obtained by a continuation on c_1.

To compare these two families of strokes, we compute in Fig.23 their geometric efficiencies and we conclude that for a given radius $r = c_1$, the corresponding stroke of the family 1 is more efficient.

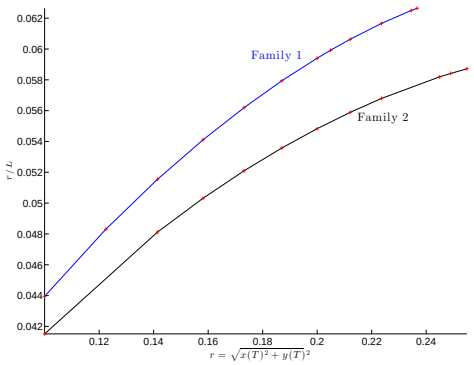

Fig. 23: Comparison of the efficiency between the two families of strokes for the true mechanical cost.

- Result of the continuation : two one-parameter families of simple loop for the mechanical cost appear and their respective efficiency is compared in Fig.23. Note that the efficiency increases with the radius of the circle c_1.

5. Conclusion

For further studies, the program is the following:

- compute a normal form of order 0 for the Purcell swimmer to complete the micro-local classification of the normal strokes,
- apply the Pontryagin Maximum Principle with the state constraints and analyze abnormal strokes,
- complete numerical results to compute strokes with larger amplitudes for the Purcell case.

Acknowledgment

J. Rouot is supported by the French Space Agency CNES, R&T action R-S13/BS-005-012 and by the région Provence-Alpes-Côte d'Azur,

References

1. A.A. Agrachev, El-H.C. Alaoui, J.-P. Gauthier, I. Kupka, Generic singularities of sub-Riemannian metrics on $\mathbb{R}^3$, *C. R. Acad. Sci. Paris Sér. I Math.* **322** 4 (1996) 377–384.
2. A.A. Agrachev, A.V. Sarychev, Strong minimality of abnormal geodesics for 2-distributions, *J. Dynam. Control Systems* **1** 2 (1995) 139–176.

3. A. Bellaïche, The tangent space in sub-Riemannian geometry, *J. Math. Sci. (New York)* n.4 **83** (1997) 461–476.
4. M. Berger, La taxonomie des courbes. Pour la science, **297** (2002) 56–63.
5. P. Bettiol, P., Bonnard, B., Giraldi, L., Martinon, P., Rouot, J., The three links Purcell swimmer and some geometric problems related to periodic optimal controls. Rad. Ser. Comp. App. **18**, Variational Methods, Ed. by M. Bergounioux et al. (2016).
6. F. Bonnans, D. Giorgi, S. Maindrault, P. Martinon, V. Grélard, *Bocop - A collection of examples, Inria Research Report, Project-Team Commands*, **8053** (2014).
7. B. Bonnard, J.-B. Caillau, E. Trélat, Second order optimality conditions in the smooth case and applications in optimal control, *ESAIM Control Optim. Calc. Var.* **13** (2007) 207–236.
8. B. Bonnard, M. Chyba, Singular trajectories and their role in control theory, Mathématiques & Applications **40**, Springer-Verlag, Berlin (2003).
9. B. Bonnard, M. Claeys, O. Cots, P. Martinon, Geometric and numerical methods in the contrast imaging problem in nuclear magnetic resonance. *Acta Appl. Math.* **135** (2015) 5–45.
10. B. Bonnard, L. Faubourg, E. Trélat, Mécanique céleste et contrôle des véhicules spatiaux. Mathématiques & Applications, Springer-Verlag **51** Berlin (2006).
11. B. Bonnard, E. Trélat, On the role of abnormal minimizers in sub-Riemannian geometry, *Ann. Fac. Sci. Toulouse Math. (6)* n. 3 **10** (2001) 405–491.
12. E. Cartan, Les systèmes de Pfaff a cinq variables et les équations aux derivées partielles du second ordre, *Ann. Sci. École Normale* **27** (1910) 109–192.
13. T. Chambrion, L. Giraldi, A. Munnier, Optimal Strokes for Driftless Swimmers: A General Geometric Approach, *Submitted* (2014).
14. O. Cots, *Contrôle optimal géométrique : méthodes homotopiques et applications*, Phd thesis, Institut Mathématiques de Bourgogne, Dijon, France (2012).
15. E. Hakavuori, E. Le Donne, Non-minimality of corners in sub-Riemannian geometry. Preprint (2015).
16. J. Happel, H. Brenner, Low Reynolds number hydrodynamics with special applications to particulate media. *Prentice-Hall, Inc., Englewood Cliffs, N.J.* (1965).
17. F. Jean, Control of Nonholonomic Systems: from Sub-Riemannian Geometry to Motion Planning, Springer International Publishing, SpringerBriefs in Mathematics (2014).
18. D.F. Lawden, Elliptic functions and applications, *Applied Mathematical Sciences*, Springer-Verlag, New York **80** (1989).
19. M. J. Lighthill, Note on the swimming of slender fish, *J. Fluid Mech.* **9** (1960) 305–317.
20. J. Lohéac, J-F. Scheid, M. Tucsnak, Controllability and time optimal control for low Reynolds numbers swimmers, *Acta Appl. Math.* **123** (2013) 175–200.
21. R. Montgomery, A tour of subriemannian geometries, their geodesics and applications. American Mathematical Society, Providence, RI. **91** (2002).
22. E. Passov, Y. Or, Supplementary notes to: Dynamics of Purcells three-link microswimmer with a passive elastic tail, *EPJ E* **35** (2012) 1–9.
23. H. Poincaré, Mémoire sur les courbes définies par une équation différentiable, *Jour. Math. Pures et Appl.* **7** 3 (1881) 375-422; **8** (1882) 251-296; **1** 4 (1885) 167-244; **2** (1886) 151-217.
24. H. Poincaré, Œuvres. Tome VII, *Éditions Jacques Gabay, Sceaux* (1996).
25. E.M. Purcell, Life at low Reynolds number, *Am. J. Phys.* **45** (1977) 3–11.
26. L. Rifford, Singulière minimisante en géométrie sous-Riemannienne, *Séminaire Bourbaki*, 68ème année, 1113 (2016), à paraître.
27. Yu.L. Sachkov, Symmetries of flat rank two distributions and sub-Riemannian struc-

tures, *Trans. Amer. Math. Soc.* n.2 **356** (2004) 457–494.
28. D. Takagi, Swimming with stiff legs at low Reynolds number, *Phys. Rev. E 92.* (2015).
29. C. Gavriel, R.B. Vinter, Second order sufficient conditions for optimal control problems with non-unique minimizers: an abstract framework, *Appl. Math. Optim.* **70** (2014) 411–442.
30. M. Zhitomirskiĭ, Typical singularities of differential 1-forms and Pfaffian equations, *American Mathematical Society, Providence, RI.* **113** (1992).